IEEE Access
Multidisciplinary | Rapid Review | Open Access Journal

Received September 7, 2020, accepted September 22, 2020, date of publication October 13, 2020,
date of current version November 6, 2020.

Digital Object Identifier 10.1109/ACCESS.2020.3030778

A Ratio-Dependent Nonlinear Predator-Prey Model With Certain Dynamical Results

ASIFA TASSADDIQ[1], (Member, IEEE), MUHAMMAD SAJJAD SHABBIR[2], QAMAR DIN[3], KHALIL AHMAD[2], AND SABEENA KAZI[1]

[1]College of Computer and Information Sciences, Majmaah University, Al Majmaah 11952, Saudi Arabia
[2]Department of Mathematics, Air University Islamabad, Islamabad 44000, Pakistan
[3]Department of Mathematics, University of Poonch Rawalakot, Azad Kashmir 12350, Pakistan

Corresponding author: Asifa Tassaddiq (a.tassaddiq@mu.edu.sa)

ABSTRACT In order to see the dynamics of prey-predator interaction, differential or difference equations are frequently used for modeling of such interactions. In present manuscript, we explore some qualitative aspects of two-dimensional ratio-dependent predator-prey model. Taking into account the non-overlapping generations for class of predator-prey system, a novel consistency preserving scheme is proposed. Our study reveals that the implemented discretization is bifurcation preserving. Some dynamical aspects including local behavior of equilibria, phase-plane analysis and emergence of Hopf bifurcation for continuous predator-prey model are studied. Moreover, existence of biologically feasible fixed points, their local asymptotic behavior and phase-plane classification of interior (positive) fixed point are carried out. Furthermore, bifurcation theory of normal forms is implemented to prove that proposed discrete-time model undergoes Neimark-Sacker bifurcation around its unique positive fixed point. Taking into account the bifurcating and fluctuating behaviour of discrete system, three chaos control strategies are implemented. Numerical simulations are provided to illustrate the theoretical discussion and effectiveness of introduced chaos control methods.

INDEX TERMS Prey-predator interaction, stability analysis, Neimark-Sacker bifurcation, chaos control.

I. INTRODUCTION

In case of continuous-time predator-prey interaction theory, differential equations are frequently used whenever it can be considered that the generation of population overlapped and fluctuate continuously in time. In contrast, when population dynamics cannot be evaluated in terms of continuous functions, a discretization is more effective to develop difference equations for the sake of getting appropriate dynamical results. The pioneer work related to the theory of predator was initiated by Lotka-Volterra model and has much limitation which is extensively perceived. Although, the functional response that indicate the rate of consumption per capita of the predator-prey models in case of system of differential equations which actually represents continuous-time models, is normally interpreted as an emphasizing behavior. Usually, the assumptions are that, predator encounter prey randomly, whereas the functional response depends upon the prosperity of prey population only, but this proposition is not constantly suitable. Thus, it is essential to upraise the functional response in population dynamics on the slow time scale at which model utilize not on the rapid behavioral time scale. Arditi and Ginzburg in [1] discuss that whenever there is a contrast between these time scales, then functional response relay on the ratio of prey to predator abundances. Moreover in [1] authors also discussed the ratio-dependent form of response function and prey dependent form with important consequences. After several laboratory observations and experimental work, the ratio-dependent theory is strongly acknowledged; see [1]–[3]. Several researchers have analyzed predator-prey models of ratio-dependence and discuss various dynamical investigations; however, these investigations either restrained errors or were only partial [4], [5]. A complete dynamical analysis had not been achieved. Although, the most challenging issue related to ratio-dependent nonlinear predator-prey models is the dynamics study of such models near origin, because such models are undefined at origin. Jost et.al., [6] discussed the analytical solution of a common ratio-dependent model at origin. Moreover, the investigation in [6] reveals that trivial equilibrium can be either saddle point or an attractor for different trajectories [6], [9]. Sarwardi et. al., considered a

The associate editor coordinating the review of this manuscript and approving it for publication was Sun Junwei.

modified ratio-dependent model with delay in predator population and examined stability conditions around biologically feasible equilibria along with bifurcation theory and parametric space [7]. Song and Zou studied a ratio-dependent predator-prey model involving diffusion [8]. Additionally, the stability of positive steady-state, Turning instability, steady state and Hopf bifurcations are examined by implementing normal form on center manifold. It is also shown that the normal form exhibit a chance of pitchfork bifurcation, see [8]. Here, we consider the following continuous-time ratio-dependent predator-prey model which was studied by several authors [6], [9], [10]:

$$\begin{cases} \dfrac{dx}{dt} = x\,(1-x) - \dfrac{axy}{x+y}, \\ \dfrac{dy}{dt} = -by + \dfrac{cxy}{x+y}. \end{cases} \tag{1}$$

Thus, x represents the population density of prey whereas population density of predator is denoted by y. Furthermore, all parameters a, b, c are positive and represents; consumption ability, death rate of predator and predator growing ability respectively. The system (1) is ratio-dependent predator-prey model in standard form and studied by various authors [4], [9]. However, Freedam [4] remonstrate that in case of biological models, the discrete-time models would certainly be more efficient and more realistic as compared to its continuous-time counterpart. Also, numerical simulation results of discrete-time models can be easily achieved and stimulate stronger dynamical results than continuous counterpart [4], [11]. Zhang considered a temporal model along with modified Holling-Tanner formalism of a ratio-dependent predator-prey model and acquire some precise existence conditions for non-constant equilibrium which confirming Turing instability [12]. Lajmiri et. al., [13] also considered system (1) with harvesting rate. They carried out both stability and bifurcation analysis with analytically and numerically. It is also shown that modified system undergoes various types of bifurcations such as Flod, Cusp, Hopf and Bogdanov-Takens bifurcations [13].

Usually, the most commonly exerted methods are piecewise constant arguments and forward Euler scheme to achieve the desire discrete-time counterparts of continuous-time models. However; these approaches are not dynamically consistent with their continuous counterparts. Jing and Yang [43] and Ushiki [52] proposed and implemented Euler forward difference method to achieve predator-prey system in discretize form and discussed bifurcation and chaos control analysis. In similar fashion, Liu and Xiao [46] considered a Lotka-Volterra model and demonstrated complex dynamics after execution of Euler approximation. For further interesting such analysis of discrete predator-prey models we referred to [33], [11], [35], [36].

Similarly, many other scholars followed by the approach of piecewise constant arguments to obtain a discrete-time predator-prey models. Jiang and Roger [42] whereas Krawcewicz and Rogers [44] applied piecewise constant arguments method and explore the competitive and cooperative case respectively. Currently, Din [39]–[41] discussed several classes of prey-predator interaction models to explore bifurcation and chaos control study by implementing piecewise constant arguments method. All these investigations ensured that there exists a dynamical inconsistency between both structures of discrete and continuous-time models.

Taking into account the consistency of dynamical characteristics, Liu and Elaydi [45] examined the predator-prey model of the type cooperative and competitive system, and Al-Kahby *et al.* [32] considered some biological systems studied dynamics of these models by applying nonstandard finite difference schemes of Mickens type [31]. In the same way, Roeger and Allen [49], and Roeger [50], [51] analyzed the dynamics of May-Leonard competitive models in discrete versions. Furthermore, Moghadas *et al.* [47] implemented nonstandard numerical scheme to analyze a Gause-type Lotka-Volterra model in generalized form. For more detail related to application of NSFD methods we refer to the study done by authors [34], [37], [38], [48].

In the present manuscript, we perform a discretization of model (1) to attain discrete-time version of continuous counterpart. Keeping in view the dynamical consistency of (1), the following discrete-time model is obtained by applying a nonstandard finite difference scheme (NSFD) of Mickens type [31]:

$$\begin{cases} \dfrac{x_{n+1}-x_n}{h} = x_n - x_{n+1}x_n - \dfrac{ax_{n+1}y_n}{x_n+y_n}; \\ \dfrac{y_{n+1}-y_n}{h} = -by_{n+1} + \dfrac{cx_ny_n}{x_n+y_n}. \end{cases} \tag{2}$$

Here, h is the step size, taking unit step size, then system (2) takes the following modified form:

$$\begin{cases} x_{n+1} = \dfrac{2x_n}{1+x_n+\frac{ay_n}{x_n+y_n}}; \\ y_{n+1} = \dfrac{y_n\left(1+\frac{cx_n}{x_n+y_n}\right)}{1+b}. \end{cases} \tag{3}$$

However, the summary of this manuscript is organized as follows:

- In section 2, we discussed the dynamics of continuous system (1).
- Section 3 is dedicated to the existence criteria of biologically suitable equilibria of system (3) and their local stability analysis is discussed with topological classification.
- In Section 4 the Neimark-Sacker bifurcation (NSB) around unique positive steady-state is carried out.
- In order to control the bifurcating and fluctuating behavior of the system under consideration, different chaos control strategies are developed in Section 5.
- In Section 6, numerical simulations are carried out in order to justify our mathematical and theoretical investigation. Concluding remarks are given at the end of this manuscript.

II. DYNAMICAL ANALYSIS OF SYSTEM (1)

Clearly, system (1) has two equilibria namely boundary equilibrium $(1, 0)$ and $\left(\frac{ab+c-ac}{c}, \frac{(c-b)(ab+c-ac)}{bc}\right)$ interior equilibrium.

The Jacobian matrix $J(1, 0)$ of system (1) about its boundary steady-state $(1, 0)$ is computed as follows:

$$J(1,0) = \begin{bmatrix} -1 & -a \\ 0 & -b+c \end{bmatrix}.$$

Clearly, $\lambda_1 = -1 < 0$ and $\lambda_2 = c - b$ are eigenvalues of $J(1, 0)$. Therefore, boundary equilibrium point is a sink if and only if $c < b$ and it is a saddle (unstable) point if and only if $c > b$. On the other hand, the Jacobian matrix of system (1) about its interior (positive) equilibrium point $\mathrm{P}_2 = \left(\frac{ab+c-ac}{c}, \frac{(c-b)(ab+c-ac)}{bc}\right)$ is computed as follows:

$$J(\mathrm{P}_2) = \begin{bmatrix} -1+a-\frac{ab^2}{c^2} & -\frac{ab^2}{c^2} \\ \frac{(b-c)^2}{c} & \frac{b(b-c)}{c} \end{bmatrix}.$$

Then, simple computation yields that $\mathrm{Det}(J(\mathrm{P}_2)) = \frac{b(c-b)(a(b-c)+c)}{c^2} > 0$ due to positivity conditions of interior equilibrium point. On the other hand, $\mathrm{Tr}(J(\mathrm{P}_2)) = a - 1 - b - \frac{ab^2}{c^2} + \frac{b^2}{c}$. Taking into account, the Routh–Hurwitz stability criterion we have P_2 is a sink if and only if $c(ac + b) < c^2(1 + b) + ab^2$. Moreover, interior equilibrium is unstable if $c(ac + b) > c^2(1 + b) + ab^2$. Moreover, system (1) undergoes Hopf bifurcation at its positive equilibrium if the parameters of system (1) belong to the following curve:

$$C_{HB} = \left\{(a, b, c) \in \mathbb{R}^3_+ : a = \frac{c\,(c+b\,(\text{c-b}))}{c^2 - b^2}, b < c, a < \frac{c}{c-b}\right\}.$$

Phase-plane classification of interior equilibrium point P_2 is depicted in **Fig. 1** in bc-plane.

To show the behavior of system (1) for selected parametric values, we take $a = 1.18$, $b = 0.15$ and $c = 0.6$. For these parametric values, the interior equilibrium point of system (1) is asymptotically stable and corresponding plots of system (1) are depicted in **Fig. 2 (a), (b)** and **(c)**.

Moreover, for $b = 0.15$ and $c = 0.6$, system (1) undergoes Hopf bifurcation as a varies in a small neighborhood of a_0 given by:

$$a_0 = \frac{c\,(c+b\,(\text{c-b}))}{c^2 - b^2} = 1.18667.$$

For $a = 1.18667$, $b = 0.15$ and $c = 0.6$ the plots of system (1) are depicted in **Fig. 3(a), (b)**and **(c)**.

III. STABILITY ANALYSIS OF SYSTEM (3)

To achieve the fixed points of system (3), we can resolve the following algebraic system of equations:

$$\begin{cases} x = \dfrac{2x}{1 + x + \dfrac{ay}{x+y}}; \\ y = \dfrac{y\left(1 + \dfrac{cx}{x+y}\right)}{1+b}. \end{cases}$$

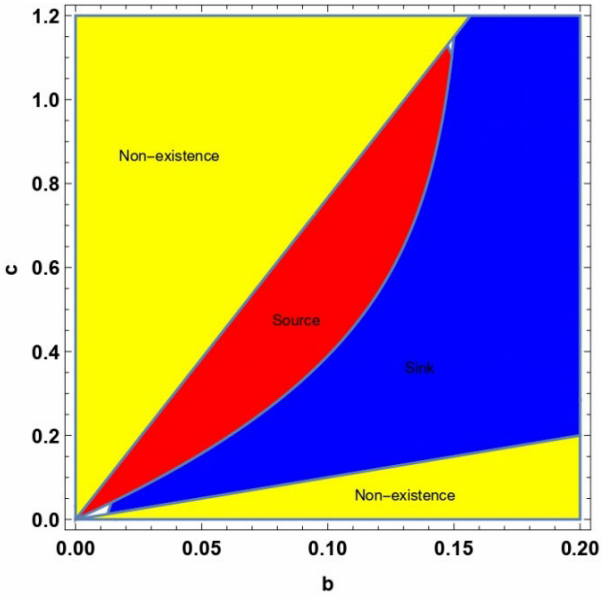

FIGURE 1. Phase-plane classification of system (1) at P_2 with a=1.15.

By simple computations, one can obtain the following equilibrium points $\mathrm{P}_1 = (1, 0)$ and $\mathrm{P}_2 = (x^*, y^*)$. Thus, boundary equilibrium point P_1 always exists, however, the unique positive (interior) equilibrium $\mathrm{P}_2 = \left(1 + a\left(\frac{b}{c} - 1\right), \frac{(c-b)(a(b-c)+c)}{bc}\right)$ for system (3) exists if and only if $ab + c > ac$.

Furthermore, the Jacobian matrix calculated at any arbitrary point (x, y) is expressed by:

$$J(x,y) = \begin{bmatrix} \frac{2(x^2+2(1+a)xy+(1+a)y^2)}{(x+x^2+y+ay+xy)^2} & -\frac{2ax^2}{(x+x^2+y+ay+xy)^2} \\ \frac{cy^2}{(1+b)(x+y)^2} & \frac{1+\frac{cx^2}{(x+y)^2}}{1+b} \end{bmatrix}$$

Now, we consider a general description related to local stability analysis of system (3). In this case, if there exists an arbitrary fixed point $\mathrm{H}^\star$ and assume that:

$$J(\mathrm{H}^\star) = \begin{bmatrix} \omega_{11} & \omega_{12} \\ \omega_{21} & \omega_{22} \end{bmatrix}$$

be the Jacobian matrix calculated at $\mathrm{H}^\star$, then the characteristic equation of $J(\mathrm{H}^\star)$ is given:

$$\mathrm{P}(\xi) = \xi^2 - \mathrm{T}\xi + \Delta,$$

where $\mathrm{T} = (\omega_{11} + \omega_{22})$, and $\Delta = \omega_{11}\omega_{22} - \omega_{12}\omega_{21}$.

For the above discussion, we obtained the following lemma 1 which describes the various conditions associated to local stability analysis of biologically feasible fixed points [30].

Lemma 3.1: Let $\mathrm{P}(\xi) = \xi^2 - \mathrm{T}\xi + \Delta$ and $\mathrm{P}(1) > 0$. Moreover, ξ_1, ξ_2 are roots of $\mathrm{P}(\xi) = 0$, then we explicate the following classical results:

(i) (i) $|\xi_1| < 1$ & $|\xi_2| < 1 \iff \mathrm{P}(-1) > 0$ and $\Delta < 1$;
(ii) (ii) $|\xi_1| > 1$ & $|\xi_2| > 1 \iff \mathrm{P}(-1) > 0$ and $\Delta > 1$;
(iii) (iii) $|\xi_1| < 1$ & $|\xi_2| > 1$ or ($|\xi_1| > 1$and $|\xi_2| < 1) \iff \mathrm{P}(-1) < 0$;

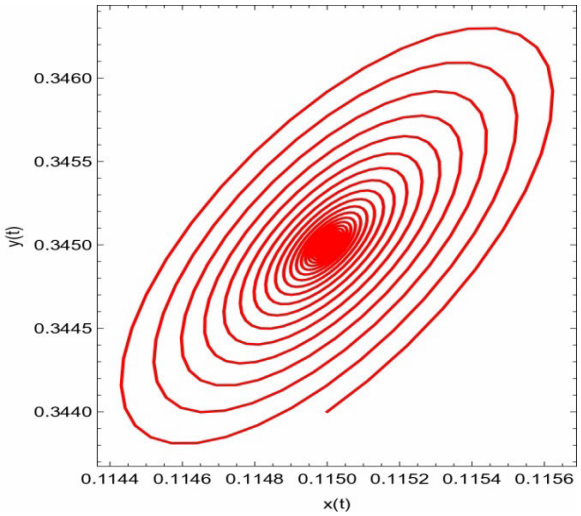

(a)

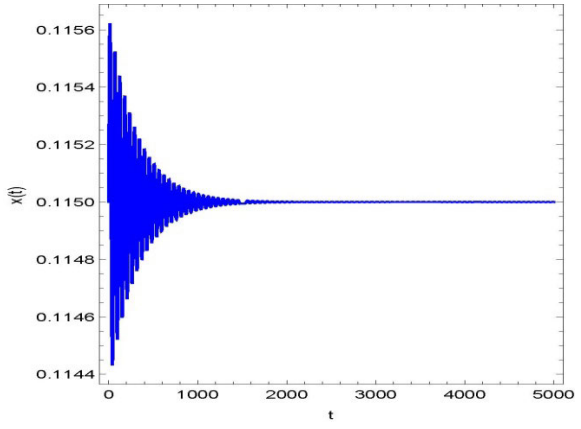

(b)

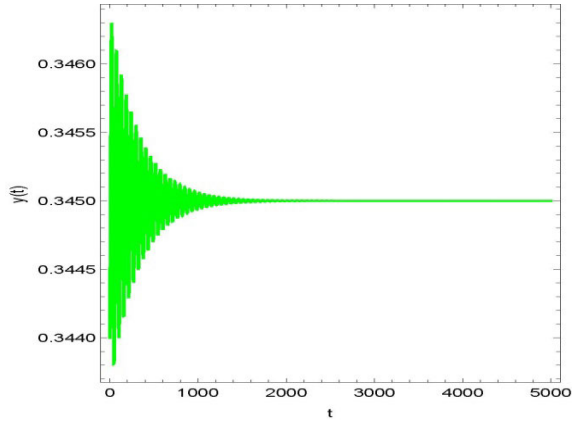

(c)

FIGURE 2. Plot for system (1) (a) Phase portrait (b) Plot for prey (c) Plot for predator.

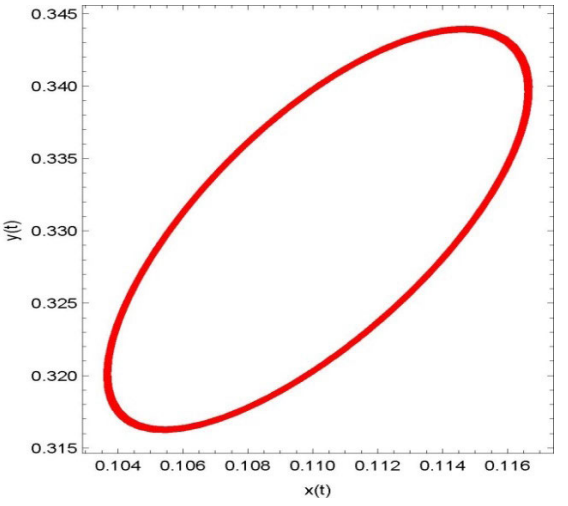

(a)

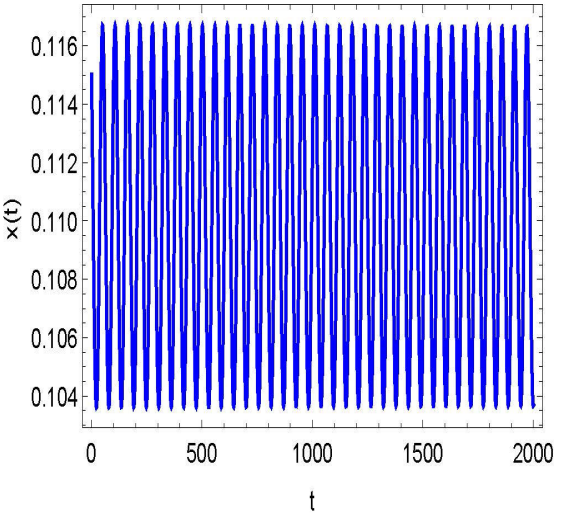

(b)

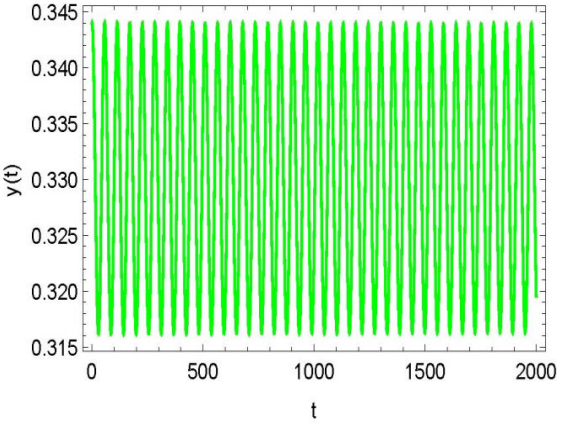

(c)

FIGURE 3. Plot for system (1) when For $a = 1.18667$, $b = 0.15$ and $c = 0.6$ (a) Phase portrait (b) Plot for prey (c) Plot for predator.

(iv) (iv) $\xi_1 = -1$ & $|\xi_2| \neq 1 \Longleftrightarrow \mathrm{P}(-1) = 0$ & $\mathrm{T} \neq 0, 2$;
(v) (v) ξ_1, ξ_2 represent complex conjugates and $|\xi_1| = 1 = |\xi_2| \Longleftrightarrow \mathrm{T}^2 - 4\Delta < 0 \text{and} \Delta = 1$;

As ξ_1, ξ_2 are eigenvalues of system (3), then we have the following topological classicification related to the stability of $\mathrm{H}^\star$.$\mathrm{H}^\star$ is known as sink if $|\xi_1| < 1$ and $|\xi_2| < 1$, as sink

is the point of suction hence stable equilibrium. H* is known as source if $|\xi_1| > 1$ & $|\xi_2| > 1$, as source is repeller hence it remains unstable. H* is known as saddle point if $|\xi_1| < 1$ and $|\xi_2| > 1$ or ($|\xi_1| > 1$ and $|\xi_2| < 1$). H* is said to be non-hyperbolic point if condition iv and v of the Lemma 3.1 is satisfied.

Now, at boundary equilibrium P_1, the variational matrix $J(P_1)$ of system (3) reduces to the following form:

$$J(P_1) = \begin{bmatrix} \frac{1}{2} & -\frac{a}{2} \\ 0 & \frac{1+c}{1+b} \end{bmatrix}.$$

Clearly, for boundary equilibrium P_1 the following assumptions hold:

- P_1 is a sink $\Longleftrightarrow c < b$.
- P_1 is saddle point for $b < c$.
- P_1 is non-hyperbolic at $b = c$.

Moreover, the variational matrix $J(P_2)$ computed at P_2 along with characteristic equation is expressed by:

$$J(P_2) = \begin{bmatrix} \frac{1}{2}\left(1 + a - \frac{ab^2}{c^2}\right) & -\frac{ab^2}{2c^2} \\ \frac{(b-c)^2}{(1+b)c} & \frac{b^2+c}{c+bc} \end{bmatrix}.$$

and

$$P(\xi) = \xi^2 - \left(\frac{1}{2}\left(1 + a - \frac{ab^2}{c^2}\right) + \frac{b^2+c}{c+bc}\right)\xi + \frac{c\left(b^2+c\right) - a\,(\text{b-c})\left(2b^2+b+c\right)}{2\,(1+b)\,c^2}, \quad (4)$$

After some usual algebraic computations, we get:

$$P(1) = \frac{b\,(\text{c-b})\,(a\,(\text{b-c}) + c)}{2\,(1+b)\,c^2} \quad (5)$$

$$P(-1) = \frac{(3+2a)\,b^2c + (3+a)\,(2+b)\,c^2 - ab^2\,(2+3b)}{2\,(1+b)\,c^2} \quad (5)$$

From (5), we see that if $ab + c > ac$, then $P(1) > 0$.

Now by using Lemma 3.1, we get the following theorem.

Theorem 3.1: Assume that $ab + c > ac$ such that P_2 represents the interior equilibrium of model (3), then the following results remains true:

- P_2 is stable (sink) $\Leftrightarrow$

$$ab^2\,(2+3b) < (3+2a)\,b^2c + (3+a)\,(2+b)\,c^2,$$

and

$$\left(ab^2 + 2c\right)(1+b) + abc^2 > abc\,(1+2b).$$

- P_2 is unstable (source) $\Longleftrightarrow$

$$(3+2a)\,b^2c + (3+a)\,(2+b)\,c^2 > ab^2\,(2+3b),$$

and

$$2c\,(1+b) + ab\left(b^2 + c^2 + b\right) < abc\,(1+2b).$$

- P_2 is saddle equilibrium $\Longleftrightarrow$

$$(3+2a)\,b^2c + (3+a)\,(2+b)\,c^2 < ab^2\,(2+3b).$$

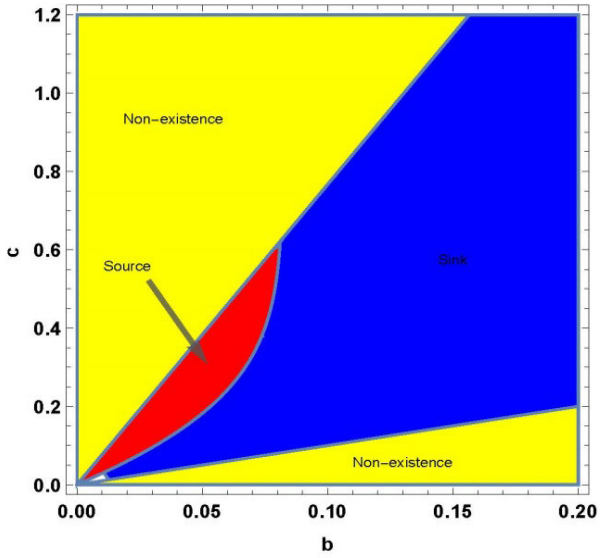

FIGURE 4. Phase-plane classification of system (3) at P_2 with a=1.15

- The interior equillibrium point P_2 of system (3) is a non-hyperbolic $\Longleftrightarrow$

$$\left|\frac{1}{2}\left(1 + a - \frac{ab^2}{c^2}\right) + \frac{b^2+c}{c+bc}\right| = \left|\frac{c(b^2+c) - a(b-c)(2b^2+b+c)}{2(1+b)c^2} + 1\right|$$

or

$$\frac{c\left(b^2+c\right) - a\,(\text{b-c})\left(2b^2+b+c\right)}{2\,(1+b)\,c^2} = 1$$

and

$$\left|\frac{1}{2}\left(1 + a - \frac{ab^2}{c^2}\right) + \frac{b^2+c}{c+bc}\right| \leq 2.$$

Phase-plane classification of interior equilibrium point P_2 of system (3) is depicted in **Fig. 4** in bc-plane.

Now compare the regions of sink and source in **Fig 5(a)** and **Fig. 5(b)** for both system (1) and system (3) for the same parametric values as given in **Fig 1** and **Fig 4**. For this, it must be noted that in Fig. 5a, source region of system (1) consists of $R1 \cup R2$, whereas source region of system (2) consists of $R2$ only. On the other hand, in Fig. 5b, sink region of system (2) consists of $R3 \cup R4$, and sink region of system (1) reduces to $R3$ only. Consequently, our novel nonstandard finite difference scheme certainly increases the stability region.

IV. NEIMARK-SACKER BIFURCATION

In this section, we investigate the existence criteria of NSB around unique positive equilibrium P_2 by considering consumption ability of prey which is $'a'$ as bifurcation parameter. For detail analysis of bifurcation in discrete-time population models, we refer to the work done by the authors [14]–[17]. Obviously, when Neimark-Sacker bifurcation exists then as a result, dynamically closed curves are appearing and attracting steady-states are unstable as varied parameter move

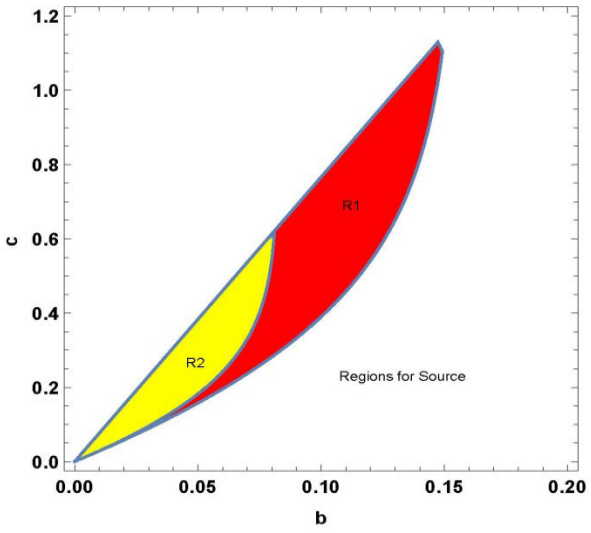

(a)

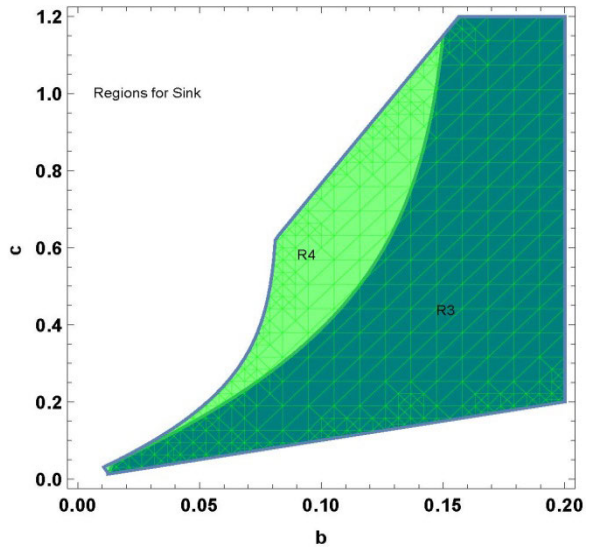

(b)

FIGURE 5. **(a) Regions for source (b) Regions for sink.**

towards the bifurcation parameter. In return, we can discover some isolated orbits along with trajectories and with periodic behavior that thickly overlay these immutable closed curves [18]. In case of non-hyperbolic steady-states, we have studied the conditions associated to system (3) and a pair of complex eigenvalues having unit modulus. For this, consider (4), then $\mathrm{P}(\xi) = 0$ has two roots which are complex conjugate and fulfill the following conditions:

$$a = \frac{c\left(b^2 - 2bc - c\right)}{(\text{b-c})\left(b + 2b^2 + c\right)},$$

and

$$\left|\frac{1}{2}\left(1 + a\left(1 - \frac{b^2}{c^2}\right) + \frac{c + b^2}{c(1+b)}\right)\right| < 2. \tag{6}$$

Suppose that

$$\psi_{\mathrm{NB}} = \left\{(a, b, c) \in R_+^3 : (6) \text{ holdwith} a = \frac{c\left(b^2 - 2bc - c\right)}{(\text{b-c})\left(2b^2 + b + c\right)}\right\}.$$

The interior steady-state P_2 of system (3) arises NSB for different parametric values belongs to a small neighborhood of the set ψ_{NB}. Let $a_1 = \frac{c(b^2-2bc-c)}{(\text{b-c})(b+2b^2+c)}$ and choosing the arbitrary parameters $(a_1, b, c) \in \psi_{\mathrm{NB}}$, then from system (3) we have the following map:

$$\begin{pmatrix} \mathrm{M} \\ \mathrm{N} \end{pmatrix} \to \begin{pmatrix} \frac{2\mathrm{M}}{1+\mathrm{M}+\frac{a_1 \mathrm{N}}{\mathrm{M+N}}} \\ \frac{\mathrm{N}\left(1+\frac{c\mathrm{M}}{\mathrm{M+N}}\right)}{1+b} \end{pmatrix} \tag{7}$$

Consider the perturbation of map (7) by choosing $\tilde{a}$ as a bifurcation parameter, we have the following map:

$$\begin{pmatrix} \mathrm{M} \\ \mathrm{N} \end{pmatrix} \to \begin{pmatrix} \frac{2\mathrm{M}}{1+\mathrm{M}+\frac{(a_1+\tilde{a})\mathrm{N}}{\mathrm{M+N}}} \\ \frac{\mathrm{N}\left(1+\frac{c\mathrm{M}}{\mathrm{M+N}}\right)}{1+b} \end{pmatrix}$$

where $|\tilde{a}| \ll 1$ is choosen as a least perturbation.

Now, we introduce the following transformations $x = \mathrm{M} - x^*$ and $y = \mathrm{N} - y^*$, where (x^*, y^*) is the interior steady-state of system (3), then map (7) is rearranged as:

$$\begin{pmatrix} x \\ y \end{pmatrix} \to \begin{pmatrix} m_{11} & m_{12} \\ m_{21} & m_{22} \end{pmatrix} \begin{pmatrix} x \\ y \end{pmatrix} + \begin{pmatrix} f_1(x, y) \\ g_1(x, y) \end{pmatrix}, \tag{8}$$

where, $f_1(x, y)$, $g_1(x, y)$, $m_{13}, m_{14}, m_{15}, m_{19}, m_{23}, m_{24}, m_{25}, m_{26}, m_{27}, m_{28}, m_{29}$, and m_{18}, as shown at the bottom of the next page,

Moreover, characteristic equation of (8) calculated at trivial fixed point can be defined as:

$$\xi^2 - \Gamma(\tilde{a})\,\xi + \Upsilon(\tilde{a}) = 0. \tag{9}$$

where

$$\Gamma(\tilde{a}) = \left(\frac{1}{2}\left(1 + (a_1 + \tilde{a}) - \frac{(a_1 + \tilde{a})b^2}{c^2}\right) + \frac{b^2 + c}{c + bc}\right),$$

$$\Upsilon(\tilde{a}) = \frac{c(b^2 + c) - (a_1 + \tilde{a})(b - c)(2b^2 + b + c)}{2(1 + b)c^2}.$$

Since $(a_1, b, c) \in \psi_{\mathrm{NB}}$, then solution of (9) are conjugate complex numbers $\xi_1, \xi_2 (|\xi_1| = |\xi_2| = 1)$. Consequently

$$\xi_1, \xi_2 = \frac{\Gamma(\tilde{a})}{2} \pm \frac{i}{2}\sqrt{4\Upsilon(\tilde{a}) - \Gamma^2(\tilde{a})}.$$

Then we obtain

$$|\xi_1| = |\xi_2| = \sqrt{\Upsilon(\tilde{a})}, \text{ impliesthat}$$

$$\left(\frac{d\,|\xi_1|}{d\tilde{a}}\right)_{(\tilde{a}=0)} = \left(\frac{d\,|\xi_2|}{d\tilde{a}}\right)_{(\tilde{a}=0)} = \frac{-(\text{b-c})\left(b + 2b^2 + c\right)}{2(1+b)c^2\sqrt{\frac{2c(b^2+c)+2(-b+c)(b+2b^2+c)a_1}{(1+b)c^2}}}.$$

Further, we assume that $\Gamma(0) := \left(\frac{1}{2}\left(1+a_1-\frac{a_1b^2}{c^2}\right)+\frac{b^2+c}{c+bc}\right) \neq 0,-1$. Moreover, $(a_1,b,c) \in \psi_{\mathrm{NB}}$ implies that $-2<\Gamma(0)<2$. Thus $\Gamma(0)\neq\pm2,0,-1$ gives $\xi_1^n,\xi_2^n \neq 1$ for all $n=1,2,3,4$ at $\tilde{a}=0$. Therefore, solutions of (9) do not overlap unit circle with coordinate axes when $\tilde{a}=0$ along with restrictions

$$\frac{1+a_1}{2}+\frac{b^2+c}{c+bc}\neq\frac{a_1b^2}{2c^2},\frac{b^2+c}{c+bc}+\frac{3+a_1}{2}\neq\frac{a_1b^2}{2c^2}. \quad (10)$$

In order to acquire the normality around $\tilde{a}=0$ of map (8), we choose $\zeta=\frac{\Gamma(0)}{2}$, $\tau=\frac{1}{2}\sqrt{4\Upsilon(0)-\Gamma^2(0)}$, and establish the following elaborations:

$$\begin{pmatrix}\frac{x}{y}\end{pmatrix}=\begin{pmatrix}m_{12} & 0\\ \zeta-m_{11} & -\tau\end{pmatrix}\begin{pmatrix}\frac{u}{v}\end{pmatrix}. \quad (11)$$

Therefore, the normal form of (8) under transformation (11) can be expressed by:

$$\begin{pmatrix}\frac{u}{v}\end{pmatrix}\to\begin{pmatrix}\zeta & -\tau\\ \tau & \zeta\end{pmatrix}\begin{pmatrix}\frac{u}{v}\end{pmatrix}+\begin{pmatrix}\frac{\tilde{f}(u,v)}{\tilde{g}(u,v)}\end{pmatrix}.$$

where

$$\begin{aligned}\tilde{f}(u,v) &= \frac{m_{13}}{m_{12}}x^2+\frac{m_{14}}{m_{12}}xy+\frac{m_{15}}{m_{12}}y^2+\frac{m_{16}}{m_{12}}x^3+\frac{m_{17}}{m_{12}}x^2y\\ &\quad+\frac{m_{18}}{m_{12}}xy^2+\frac{m_{19}}{m_{12}}y^3+O\left((|u|+|v|)^4\right),\\ \tilde{g}(u,v) &= \left(\frac{(\zeta-m_{11})m_{13}}{\tau m_{12}}-\frac{m_{23}}{\tau}\right)x^2\\ &\quad+\left(\frac{(\zeta-m_{11})m_{14}}{\tau m_{12}}-\frac{m_{24}}{\tau}\right)xy\\ &\quad+\left(\frac{(\zeta-m_{11})m_{15}}{\tau m_{12}}-\frac{m_{25}}{\tau}\right)y^2\end{aligned}$$

$$\begin{aligned}f_1(x,y) &= m_{13}x^2+m_{14}xy+m_{15}y^2+m_{16}x^3+m_{17}x^2y\\ &\quad+m_{18}xy^2+m_{19}y^3+O\left((|x|+|y|+|\tilde{a}|)^4\right);\\ g_1(x,y) &= m_{23}x^2+m_{24}xy+m_{25}y^2+m_{26}x^3+m_{27}x^2y\\ &\quad+m_{28}xy^2+m_{29}y^3+O\left((|x|+|y|+|\tilde{a}|)^4\right);\\ m_{13} &= \frac{\tilde{a}^2b^4-2\tilde{a}^2b^2c^2+\tilde{a}^2c^4+2\tilde{a}cb^3-2\tilde{a}b^2c^2-c^4}{4c^3(\tilde{a}(b-c)+c)};\\ m_{14} &= \frac{\tilde{a}b^2\left(\tilde{a}b^2+2bc-\tilde{a}c^2-c^2\right)}{2c^3\left(\tilde{a}\,(\mathrm{b\text{-}c})+c\right)};\\ m_{15} &= \frac{\tilde{a}b^3\left(\tilde{a}b+2c\right)}{4c^3\left(\tilde{a}\,(\mathrm{b\text{-}c})+c\right)};\\ m_{19} &= \frac{-\tilde{a}b^4\left(\tilde{a}^2b^2+4\tilde{a}bc+4c^2\right)}{8c^4\left(\tilde{a}\,(\mathrm{b\text{-}c})+c\right)^2};\\ m_{23} &= \frac{-b\,(\mathrm{b\text{-}c})^2}{c\,(1+b)\,(\tilde{a}b-\tilde{a}c+c)};\\ m_{24} &= \frac{-2b^2\,(\mathrm{b\text{-}c})}{c\,(1+b)\,(\tilde{a}b-\tilde{a}c+c)};\\ m_{25} &= \frac{-b^3}{c\,(1+b)\,(\tilde{a}b-\tilde{a}c+c)};\\ m_{26} &= \frac{b^2\,(\mathrm{b\text{-}c})^2}{c\,(1+b)\,(\tilde{a}b-\tilde{a}c+c)};\\ m_{27} &= \frac{b^2\,(\mathrm{b\text{-}c})\,(3b-c)}{c\,(1+b)\,(\tilde{a}b-\tilde{a}c+c)};\\ m_{28} &= \frac{(3b-2c)b^3}{c\,(1+b)\,(\tilde{a}b-\tilde{a}c+c)};\\ m_{29} &= \frac{b^4}{c\,(1+b)\,(\tilde{a}b-\tilde{a}c+c)};\\ m_{18} &= \frac{-\tilde{a}b^3\left(3\tilde{a}^2b^3-3\tilde{a}^2bc^2+12\tilde{a}b^2c-3\tilde{a}bc^2-4\tilde{a}c^3+12bc^2-4c^3\right)}{8c^4\left(\tilde{a}\,(\mathrm{b\text{-}c})+c\right)^2};\end{aligned}$$

$$+\left(\frac{(\zeta-m_{11})\,m_{16}}{\tau m_{12}}-\frac{m_{26}}{\tau}\right)x^3$$
$$+\left(\frac{(\zeta-m_{11})\,m_{17}}{\tau m_{12}}-\frac{m_{27}}{\tau}\right)x^2y$$
$$+\left(\frac{(\zeta-m_{11})\,m_{18}}{\tau m_{12}}-\frac{m_{28}}{\tau}\right)xy^2$$
$$+\left(\frac{(\zeta-m_{11})\,m_{19}}{\tau m_{12}}-\frac{m_{29}}{\tau}\right)y^3+O\left((|u|+|v|)^4\right),$$

$x = m_{12}u$ and $y = (\zeta - m_{11})\,u - \tau v$. Now, we define $\mathbf{L} \neq 0$ belongs to the set of real numbers as follows:

$$\mathbf{L} = \left(\left[-\mathbf{Re}\left(\frac{(1-2\xi_1)\xi_2^2}{1-\xi_1}\Omega_{20}\Omega_{11}\right)-\frac{1}{2}|\Omega_{11}|^2+|\Omega_{02}|^2 +\mathbf{Re}\,(\xi_2\Omega_{21})\right]\right)_{\tilde{a}=0}.$$

where

$$\Omega_{11} = \frac{1}{4}\left[\tilde{f}_{uu}+\tilde{f}_{vv}+i(\tilde{g}_{uu}+\tilde{g}_{vv})\right].$$
$$\Omega_{02} = \frac{1}{8}\left[\tilde{f}_{uu}-\tilde{f}_{vv}-2\tilde{g}_{uv}+i(\tilde{g}_{uu}-\tilde{g}_{vv}+2\tilde{f}_{uv})\right].$$
$$\Omega_{20} = \frac{1}{8}\left[\tilde{f}_{uu}-\tilde{f}_{vv}+2\tilde{g}_{uv}+i(\tilde{g}_{uu}-\tilde{g}_{vv}-2\tilde{f}_{uv})\right].$$
$$\Omega_{21} = \frac{1}{16}\left[\tilde{f}_{uuu}+\tilde{f}_{uvv}+\tilde{g}_{uuv}+\tilde{g}_{vvv}+i(\tilde{g}_{uuu}+\tilde{g}_{uvv}-\tilde{f}_{uuv}-\tilde{f}_{vvv})\right].$$

The aforemention detail mathematical investigation, one can express the following theorem [19]–[23].

Theorem 4.1: There exists a NSB around interior equilibrium $P_2 := (x^*, y^*)$ *whenever,* $'a'$ *deviates in a least neighborhood of* $a_1 := \frac{c(b^2-c(1+2b))}{(2b^2+b+c)(b-c)}$. *In addition, if* $\mathbf{L} < \mathbf{0}$, $(\mathbf{L} > \mathbf{0})$, *respectively, then an attracting (or repelling) invariant closed curve flacutate from* $P_2 := (x^*, y^*)$ *respectively for* $a > a_1 (or\, a < a_1)$.

V. CHAOS CONTROL ANALYSIS

The chaos control and theory of bifurcation is one of the most vital and developed area of the current research. It has significant characteristics in population model, especially the models corresponding to the ecology and mathematical biology exploring biological breeding of species. As compared to continuous-time population models, the behaviour of discrete-time population models are most chaotic and complex. Consequently, chaotic and fluctuating behaviors are considered to be harmful and capable to create alarming situations for interacting biological species. In order to achieve stability behavior in the dynamics of interacting species, chaos control methods are implemented. For implementation of chaos control techniques, a small perturbation is added to given chaotic system in such a way that both given and perturbed (controlled) systems are steady-states preserving. Usually, state feedback control and parameter perturbation are applied to obtain new controlled system corresponding to given chaotic system.

The present section consists of the following feedback control techniques to control unusual and unstable behavior of trajectory towards stable one, that is,

- OGY feedback control strategy
- Hybrid feedback control strategy
- An exponential type control strategy

A. OGY CONTROL METHOD

Here, we execute the OGY control method proposed by Ott *et al.*, see also [24], [25]. Now, we implement OGY method to system (3). Consequently, we have achieved the modification of (3) as follows:

$$\left.\begin{aligned} x_{n+1} &= \frac{2x_n}{1+x_n+\frac{ay_n}{x_n+y_n}} = f\,(x_n, y_n, a)\\ y_{n+1} &= \frac{y_n\left(1+\frac{cx_n}{x_n+y_n}\right)}{1+b} = g\,(x_n, y_n, a)\end{aligned}\right\} \tag{12}$$

where a is taken as a control parameter. Here, we restrict a to a small interval $a \in (a_0-\varepsilon, a_0+\varepsilon)$ to achieve desire control by implementing a small perturbations. Also a_0 indicates any arbitrary value from chaotic region. Our aim is to shift the uncertain trajectory towards the desire orbit. For this, we implement the stabilizing feedback control strategy. Moreover, consider that (x^*, y^*) be an unstable steady-state of model (3) from the chaotic region under the influence of NSB, then by applying the following linear map, the system (12) can be evaluated in the neighbourhood of (x^*, y^*) as follows:

$$\begin{bmatrix} x_{n+1}-x^* \\ y_{n+1}-y^* \end{bmatrix} \approx \mathrm{A}\left(x^*, y^*, a_0\right)\begin{bmatrix} x_n-x^* \\ y_n-y^* \end{bmatrix} + \mathrm{B}\,[a-a_0] \tag{13}$$

where

$$\mathrm{A}\left(x^*, y^*, a_0\right) = \begin{bmatrix} \frac{\partial f(x^*,y^*,a_0)}{\partial x} & \frac{\partial f(x^*,y^*,a_0)}{\partial y} \\ \frac{\partial g(x^*,y^*,a_0)}{\partial x} & \frac{\partial g(x^*,y^*,a_0)}{\partial y} \end{bmatrix} = \begin{bmatrix} \frac{1}{2}\left(1+a_0-\frac{a_0b^2}{c^2}\right) & -\frac{a_0b^2}{2c^2} \\ \frac{(b-c)^2}{(1+b)c} & \frac{b^2+c}{c+bc} \end{bmatrix}$$

and

$$\mathrm{B} = \begin{bmatrix} \frac{\partial f(x^*,y^*,a_0)}{\partial a} \\ \frac{\partial g(x^*,y^*,a_0)}{\partial a} \end{bmatrix} = \begin{bmatrix} \frac{(b-c)(a_0(b-c)+c)}{2c^2} \\ 0 \end{bmatrix}$$

Moreover, the controllable system (12) yields the following matrix $C = [\mathrm{B} : \mathrm{AB}]$ is of rank 2.

Moreover, taking $[a-a_0] = -Q\begin{bmatrix} x_n-x^* \\ y_n-y^* \end{bmatrix}$, where $Q = \begin{bmatrix} k_1 & k_2 \end{bmatrix}$, then system (13) can be written as

$$\begin{bmatrix} x_{n+1}-x^* \\ y_{n+1}-y^* \end{bmatrix} \approx [\mathrm{A}-\mathrm{B}Q]\begin{bmatrix} x_n-x^* \\ y_n-y^* \end{bmatrix}$$

Furthermore, the equivalent controlled system of (3) is stated as:

$$\left.\begin{aligned} x_{n+1} &= \frac{2x_n}{1+x_n+\frac{y_n}{x_n+y_n}[a_0-k_1(x_n-x^*)-k_2(y_n-y^*)]}\\ y_{n+1} &= \frac{y_n\left(1+\frac{cx_n}{x_n+y_n}\right)}{1+b}.\end{aligned}\right\} \tag{14}$$

Moreover, the equilibrium point (x^*, y^*) is asymptotically stable when both eigenvalues of $''\mathrm{A}-\mathrm{B}Q''$ belongs to an open

unit disk. The characteristic equation of the variational matrix $''A - BQ''$ of the map (14) is expressed by:

$$P(\xi) = \xi^2 - T_1\xi + D_1 = 0,$$

where

$$D_1 = \frac{(b-c)^3 ck_2 + a(b-c)(k_2(b-c)^3 - c(b+2b^2+c)}{2(1+b)c^3} + \frac{c(b^2+c)(c-bk_1+ck_1)}{2(1+b)c^3} + \frac{(c-b)(b^2+c)k_1)}{2(1+b)c^3};$$

$$T_1 = \frac{b^2+c}{c+bc} + \frac{c^2-(b-c)(ck_1+a(b+c+(\text{b-c})k_1))}{2c^2}.$$

Furthermore, the marginal lines representing region of stability can be evaluated as follows:

$$L_1 : P(1) = 0,$$
$$L_2 : P(-1) = 0,$$
$$L_3 : P(0) = 1.$$

B. HYBRID CONTROL METHOD

In this section, we apply a Hybrid feedback control strategy to control chaos which is produced by Neimark-Sacker bifurcation [26]. This strategy was first applied to control the chaos which is developed under the emergence of period-doubling bifurcation, but on the other hand, similar methodology is adopted for control the NSB [27]. Suppose that system (3) undergoes Neimark-Sacker bifurcation at (x^*, y^*), then modified hybrid control map can be formulated by:

$$\begin{cases} x_{n+1} = \varsigma\left[\dfrac{2x_n}{1+x_n+\frac{ay_n}{x_n+y_n}}\right] + (1-\varsigma)x_n \\ y_{n+1} = \varsigma\left[\dfrac{y_n\left(1+\frac{cx_n}{x_n+y_n}\right)}{1+b}\right] + (1-\varsigma)y_n. \end{cases} \tag{15}$$

Here, controlled parameter $\varsigma \in (0, 1)$. It is observed that the map (15) comprises of feedback control as well as parameter perturbation. Further noticed that for suitable selection of parametric value of ς, the bifurcation for interior steady-state (x^*, y^*) can be advanced (delayed) or indeed totally eradicated, for more detail we refer to references therein [28], [29]. Furthermore, the Jacobian of system (15) estimated at (x^*, y^*) is specified by:

$$\begin{bmatrix} \frac{1}{2}\left(2+\left(a-1-\frac{ab^2}{c^2}\right)\varsigma\right) & -\frac{ab^2\varsigma}{2c^2} \\ \frac{(b-c)^2\varsigma}{(1+b)c} & 1+\frac{b(b-c)\varsigma}{(1+b)c} \end{bmatrix},$$

and characteristic equation takes the form

$$\xi^2 - T_2\xi + D_2 = 0,$$

where

$$T_2 = \frac{1}{2}\left(4+\left(a-1-\frac{ab^2}{c^2}\right)\varsigma + \frac{2b(\text{b-c})\varsigma}{(1+b)c}\right),$$

$$D_2 = -\frac{c^2(b(\varsigma-1)-1)(2+(a-1)\varsigma)+b^2c\varsigma(\varsigma-2(1+a\varsigma))}{2(1+b)c^2} - \frac{ab^2\varsigma(1+b(1+\varsigma))}{2(1+b)c^2}.$$

Analogous to aforementioned mathematical computation, we deduced the following lemma associated to the local stability of (15) around (x^*, y^*).

Lemma 5.1: The interior fixed point (x^*, y^*) of controlled map (15) is locally asymptotically stable, whenever the following condition satisfied:

$$|T_2| < 1 + D_2 < 2.$$

C. EXPONENTIAL TYPE CONTROL METHOD

Now we develop an Exponential type control method proposed by Din [54] for system (3):

$$\begin{aligned} x_{n+1} &= e^{-s_1(x_n-x^\star)}\left[\frac{2x_n}{1+x_n+\frac{ay_n}{x_n+y_n}}\right] \\ y_{n+1} &= e^{-s_2(y_n-y^\star)}\left[\frac{y_n\left(1+\frac{cx_n}{x_n+y_n}\right)}{1+b}\right] \end{aligned} \tag{16}$$

where, s_1 and s_2 are control parameters for system (16). The characteristic equation of system (16) is given by

$$\xi^2 - (\tau_{11}+\tau_{22})\xi + \tau_{11}\tau_{22} - \tau_{12}\tau_{21} = 0,$$

where

$$\tau_{11} = \text{Exp}\left(2ar\left(1-\frac{b}{c}\right)\right) \times \frac{\left(c^2(1-2r) - a(\text{b-c})(b+c+2cr)\right)}{2c^2};$$

$$\tau_{22} = \frac{b^2+c}{c(1+b)} + \frac{(b-c)(a(b-c)+c)s}{bc};$$

$$\tau_{12} = \frac{-ab^2}{2c^2}\text{Exp}\left(2ar\left(1-\frac{b}{c}\right)\right); \tau_{21} = \frac{(b-c)^2}{(1+b)c}.$$

Lemma 5.2: The equilibrium $(x^\star, y^\star)$ of the controlled system (16) is locally asymptotically stable, if

$$|\tau_{11}+\tau_{22}| < 1 + \tau_{11}\tau_{22} - \tau_{12}\tau_{21} < 2.$$

VI. NUMERICAL SIMULATION

This particular section contains some numerical simulations which are provided to verify our theoretical and mathematical discussions. It is noted that the parametric values selected randomly. First figure **Fig. 6(a) &(b)** shows that system (3) undergoes NSB in both prey and predator population respectively. The maximum Lyapunov exponent is depicted in **Fig. 6(c).** Similarly **Fig. 6(d)** illustrates the controllable region using OGY control method. From **Fig. 6(e, f)** it is clear that hybrid control strategy successfully controls the bifurcation whereas **Fig. 6(g)** represents controllable stability region for system (16). Moreover, to show interesting behaviours of system (3), some phase portraits are plotted in **Fig. 7**.

Example 6.1: Let $b = 1.8$, $c = 2.8$, $a \in [2.2, 2.6]$ and with initial conditions $(x_0, y_0) = (0.12, 0.07)$, then in system (3)

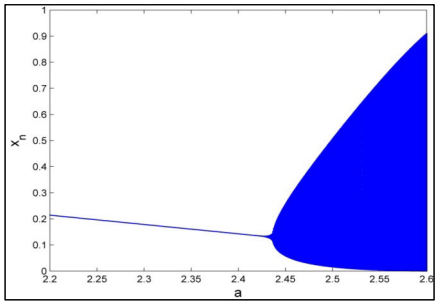

(a)

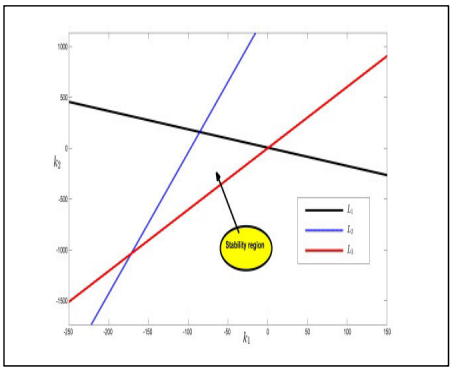

(d)

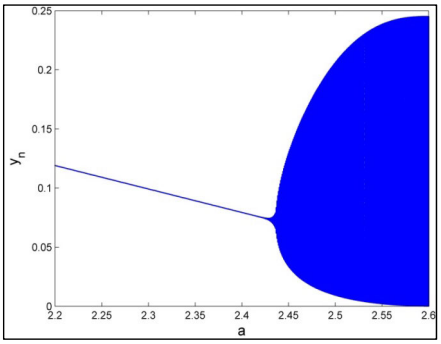

(b)

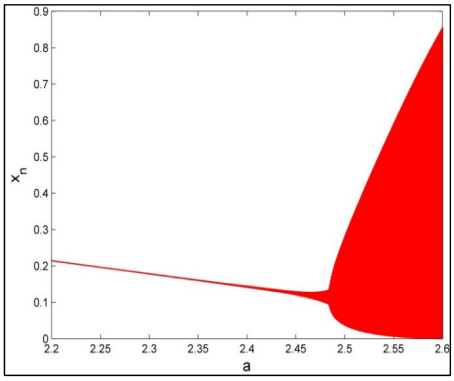

(e)

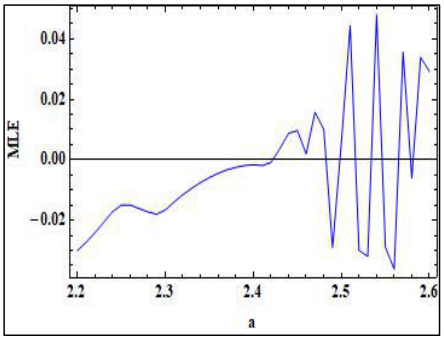

(c)

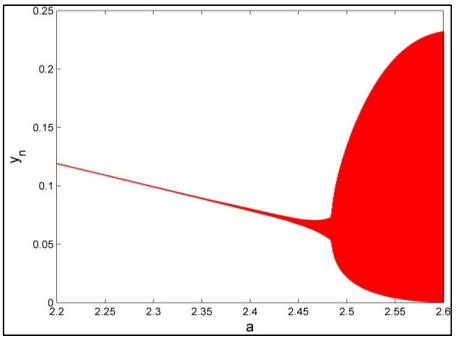

(f)

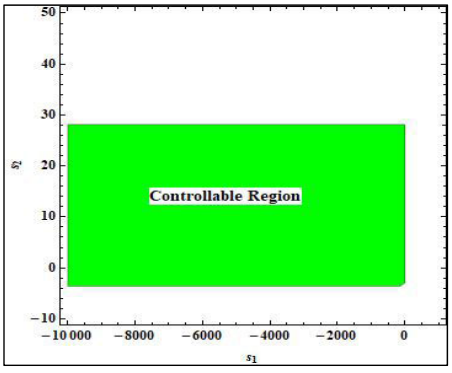

(g)

FIGURE 6. Bifurcation diagrams and MLE for system (3) with $\mathbf{b = 1.8}$, $\mathbf{c = 2.8}$, $\mathbf{a \in [2.2, 2.6]}$ and $\mathbf{(x_0, y_0) = (0.12, 0.07)}$; (a) Bifurcation diagram for $\mathbf{x_n}$ (b) Bifurcation diagram for $\mathbf{y_n}$ (c) MLE (d) Stability region for controlled system (14). (e) and (f) represents bifurcation diagrams of prey and predator population respectively, for controlled system (18) when $\varsigma = 0.0893$. (g) Stability region for controlled system (16).

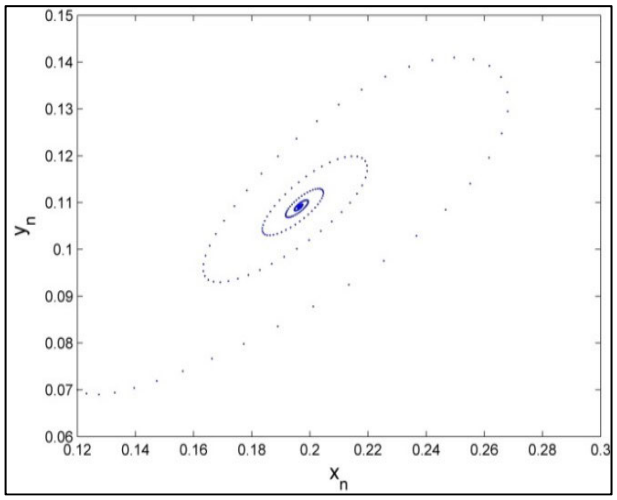

(a) $a = 2.25$

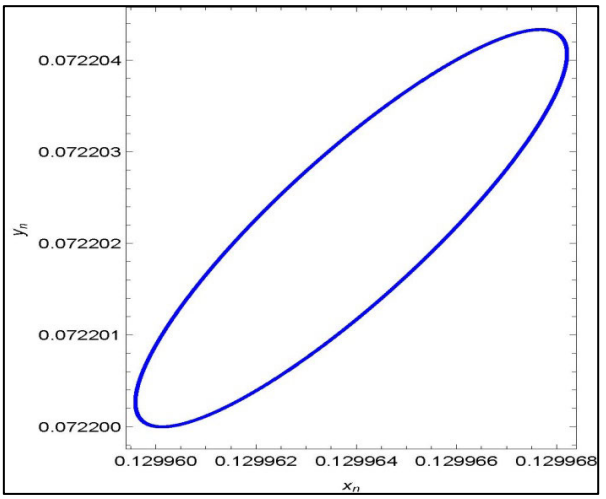

(d) $a = 2.4361010830324914$

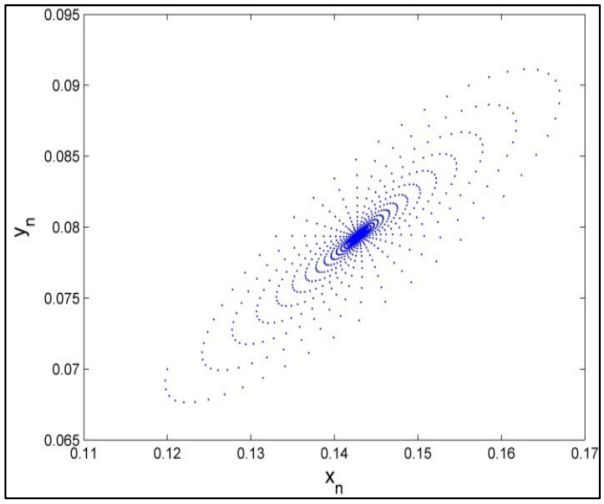

(b) $a = 2.4$

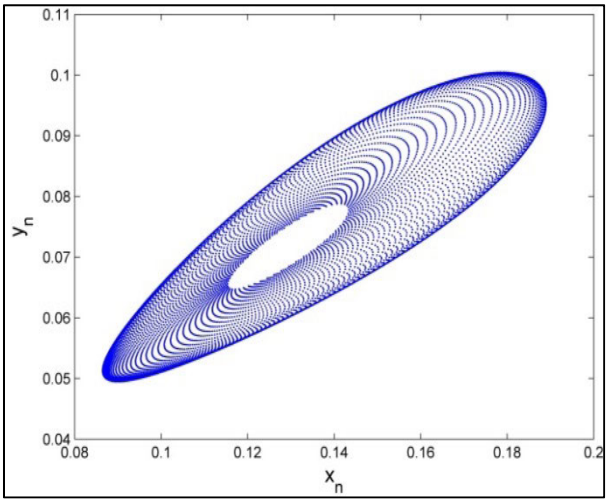

(e) $a = 2.44$

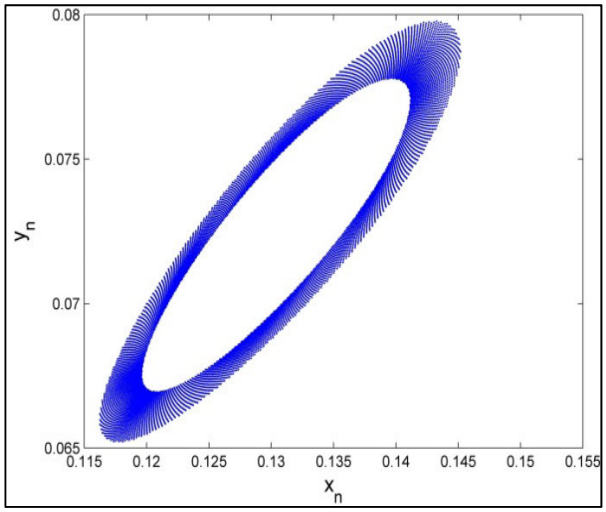

(c) $a = 2.4361$

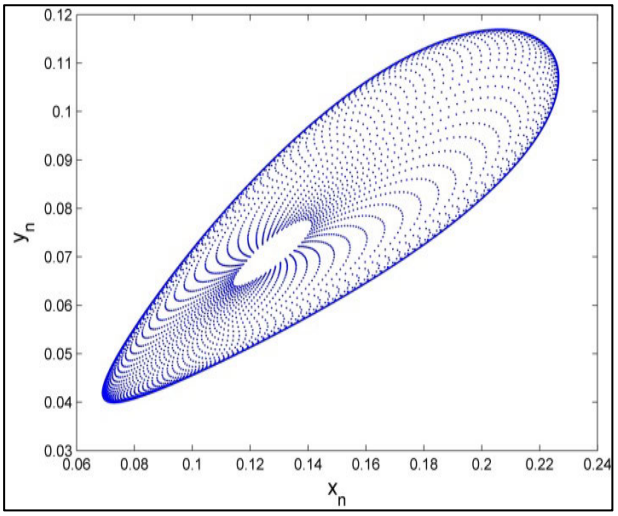

(f) $a = 2.445$

FIGURE 7. Phase portraits of system (3) for different values of bifurcation parameter a.

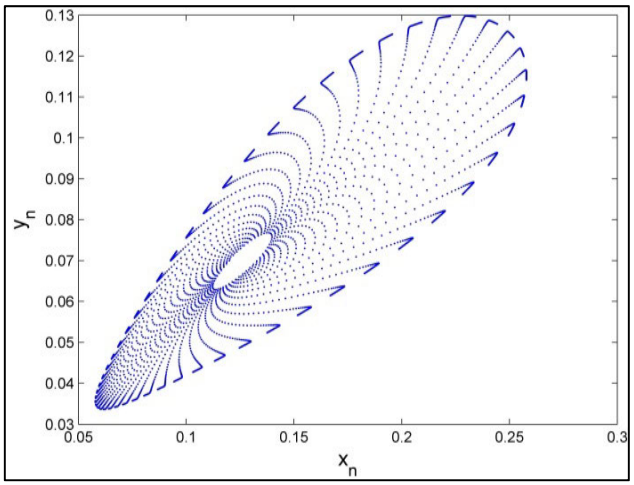

(g) $a = 2.45$

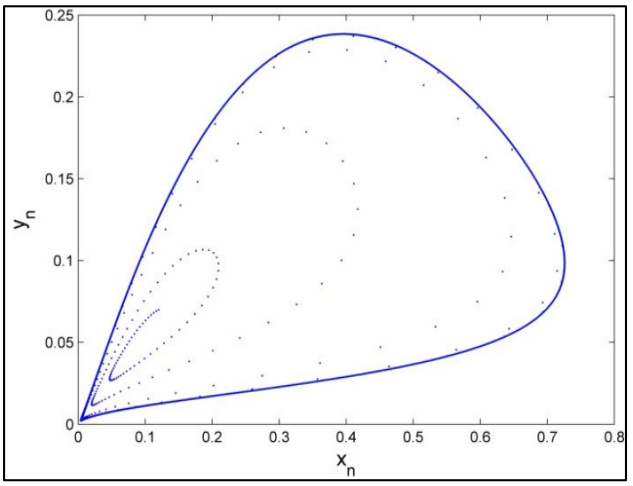

(h) $a = 2.55$

FIGURE 7. ***(Continued.)*** **Phase portraits of system (3) for different values of bifurcation parameter a.**

NSB appears whenever $a \approx 2.4361010830324914$. On the other hand, the parallel bifurcation diagrams of prey and predator populations along with MLE are plotted in **Fig. 6** (**a**, **b**, **c**). Furthermore, the map (3) has an interior equilibrium point $(x^*, y^*) = (0.1299638, 0.07220216)$ with characteristic equation calculated by

$$\xi^2 - 1.9850806748692\xi + 1.000000002=0 \qquad (17)$$

Furthermore, the roots of (17) are $\xi_1 = 0.9925403374346128 - 0.12191668698412544i$ and $\xi_2 = 0.9925403374346128+0.12191668698412544i$ with $|\xi_{1,2}|= 1$. Thus the parameters $(a, b, c) = (2.4361010830324914, 1.8, 2.8) \in \psi_{\mathrm{NB}}$.

Next, we implement OGY control strategy for controlling the chaos which is due to appearance of NSB. For this, taking $a = 2.4361, b = 1.8, c = 2.8$, and unique positive equilibrium $(x^*, y^*) = (0.12996, 0.0722)$, then Jacobian matrix $\mathrm{A} - \mathrm{B}Q$ of modified controlled system (14) is reduces to

$$\mathrm{A} - \mathrm{B}Q := \begin{bmatrix} 1.214673 + 0.0232079k_1 & -0.50338 + 0.02321k_2 \\ 0.12755102040816318 & 0.7704081632653061 \end{bmatrix}.$$

Moreover, the marginal stability lines L_1, L_2 and L_3 are given by

$$\begin{aligned} \mathrm{L}_1 &\to k_2 = -1.8k_1 + 5.04, \\ \mathrm{L}_2 &\to k_2 = 13.88k_1 + 1346.23, \\ \mathrm{L}_3 &\to k_2 = 6.04k_1. \end{aligned}$$

However, stability region bounded by L_1, L_2 and L_3 is plotted in **Fig. 6(d).**

Furthermore, we again take $b = 1.8, c = 2.8, a \in [2.2, 2.6]$ with initial conditions $(x_0, y_0) = (0.12, 0.07)$. For these values of parameters, system (3) undergoes NSB. Now we perform hybrid control strategy for the purpose of controlling chaos. For above parametric values, the modified controlled map (15) takes the form:

$$\begin{aligned} x_{n+1} &:= \varsigma \left[\frac{2x_n}{1 + x_n + \frac{2.4361y_n}{x_n+y_n}} \right] + (1 - \varsigma)\, x_n \\ y_{n+1} &:= \varsigma \left[\frac{y_n \left(1 + \frac{2.8x_n}{x_n+y_n}\right)}{1 + 1.8} \right] + (1 - \varsigma)\, y_n. \end{aligned} \qquad (18)$$

TABLE 1. **Controllable interval for system (18) with various values of bifurcation parameter a in chaotic region.**

Values of $'a'$ from chaotic region	Stability interval of $'\varsigma'$
2.44	$0 < \varsigma < 0.93333333333333$
2.46	$0 < \varsigma < 0.56732026143791$
2.47	$0 < \varsigma < 0.36767676767677$
2.48	$0 < \varsigma < 0.15555555555555$
2.482	$0 < \varsigma < 0.11153039832284$
2.483	$0 < \varsigma < 0.08930949877322$

The interval of stability for system (18) can be seen in the following Table 1 when different values of bifurcation parameter a belong to chaotic region:

The bifurcation controlled diagrams of model (18) are displayed in **Fig. 6(e, f)**. Similarly for above parametric values defined in example 6.1, the controllable portion of stability by applying map (16) is plotted in **Fig. 6(g).**

In Fig. 8, some phase portraits of system (3) are plotted, whenever bifurcation parameter a takes the different values from chaotic region with initial conditions $(x_0, y_0) = (0.12, 0.07)$, while parameters $b = 1.8, c = 2.8$ are remain fixed for each case.

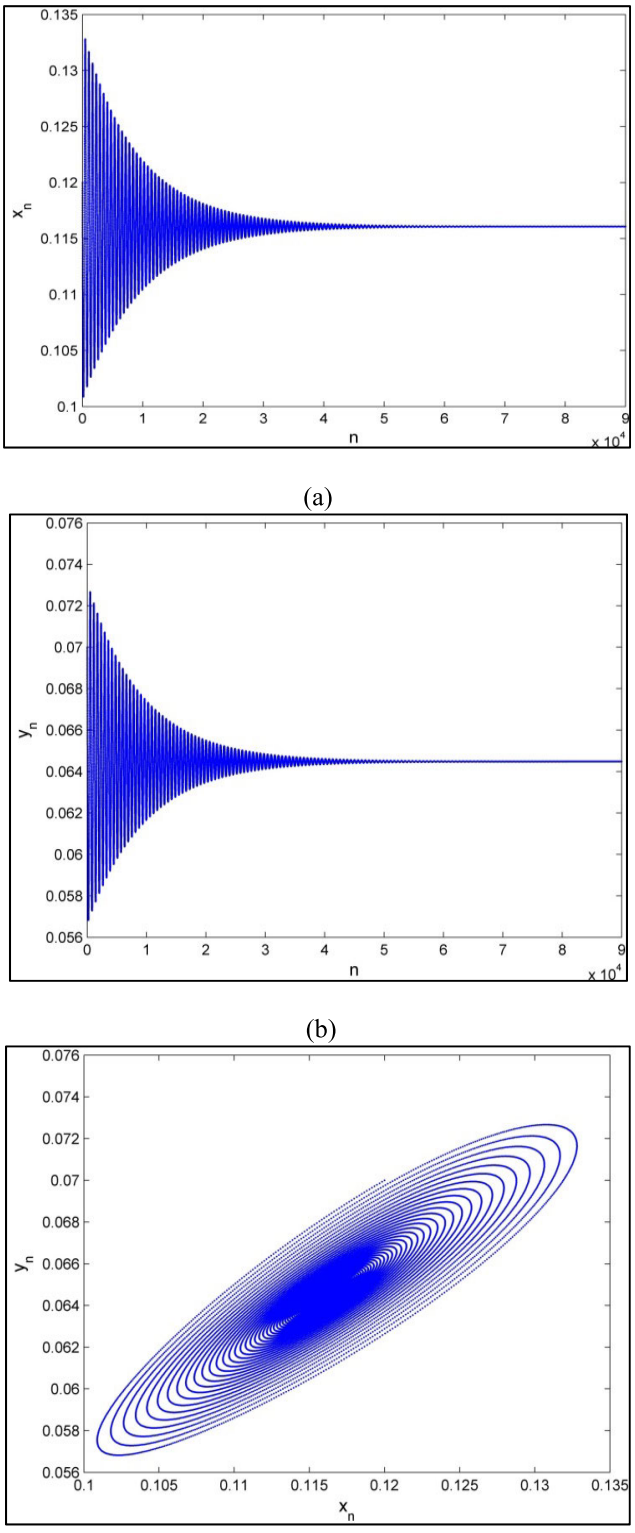

FIGURE 8. Plots for controlled map (18) when $\varsigma = 0.0893$ and $a = 2.475$ (a) Plot of prey population (b) Plot of predator population (c) Phase portrait.

VII. CONCLUSION

We discuss the dynamics of a ratio-dependent predator-prey model. A nonstandard finite difference scheme is implemented for discretization in order to obtain system (3). Moreover, this scheme of discretization is more effective and reliable as compared to Euler forward difference scheme used in [10]. It is observed that system (1) has two fixed points $P_1 = (1, 0)$ and $P_2 = (x^*, y^*)$. The linearization approach is used to achieve the local stability conditions of P_1 and P_2 whereas plots for system (1) plotted in **Fig. 2** and **Fig. 3** described stability analysis. Furthermore, the given system has unique positive fixed point $P_2 ac < ab + c$. The topological classification of P_2 for system (1) and system (3) has shown in **Fig. 1** and **Fig. 4**. It is proved that system (1) undergoes Hopf bifurcation at P_2 whereas system (3) undergoes Neimark-Sacker bifurcation at P_2 by applying bifurcation theory of normal form. Also, our mathematical investigations are supported by some figures. Neimark-Sacker bifurcation diagrams of system (3) is depicted for different values of parameters say $b = 1.8, c = 2.8, a \in [2.2, 2.6]$ along with initial conditions $(x_0, y_0) = (0.12, 0.07)$, then one can easily observe that $P_2 = (0.1299638, 0.07220216)$ is stable for $a < 2.4361010830324914$ and loses its stability at $a = 2.4361010830324914$, in this case system (3) undergoes Neimark-Sacker bifurcation when consumption ability a exceed the value 2.4361010830324914 also an attracting invariant closed curves appears when $a > 2.4361010830324914$. **Fig. 6(a), 6(b)** and **6(c)** represents the bifurcation diagrams and MLE for system (3). Furthermore, **Fig. 6(d), 6(e), 6(f)** and **6(g)** verify that our proposed control techniques control bifurcation successfully. Additionally, an interesting comparison plot of sink and source region for both differential equation model (1) and difference equation model (3) are depicted in **Fig. 5**. Different phase portraits in **Fig. 7** for various values of bifurcation parameter show the behavioral change in system. At the end, plot and phase portrait for controlled system (18) depicted in **Fig. 8** ensures that system has restore the stability region. From the above discussion we also say that consumption ability in predator-prey population has dynamical and remarkable consequences for stability of population models.

VIII. FUTURE DIRECTION

It is clear that the functional response in system (1) is of Holling type-II function. Therefore, it is more interesting to develop Holling type-III functional response. The dynamics of ratio-dependent predator-prey model (1) with Holling type-III functional response is our future work for investigation.

Moreover, it is also interesting to implement biologically feasible impulsive effects on predator-prey interaction and to apply techniques based on numerical computation of the Poincare map [55].

REFERENCES

[1] R. Arditi and L. R. Ginzburg, "Coupling in predator-prey dynamics: Ratio-dependence," *J. Theor. Biol.*, vol. 139, no. 3, pp. 311–326, Aug. 1989.
[2] R. Arditi, L. R. Ginzburg, and H. R. Akcakaya, "Variation in plankton densities among lakes: A case for ratio-dependent predation models," *Amer. Naturalist*, vol. 138, no. 5, pp. 1287–1296, Nov. 1991.

[3] I. Hanski, "The functional response of predator: Worries about scale," in *Proc. TREE*, 1991, pp. 141–142.
[4] H. I. Freedman and R. M. Mathsen, "Persistence in predator-prey systems with ratio-dependent predator influence," *Bull. Math. Biol.*, vol. 55, no. 4, pp. 817–827, Jul. 1993.
[5] Y. Kuang and E. Beretta, "Global qualitative analysis of a ratio-dependent predator-prey system," *J. Math. Biol.*, vol. 36, no. 4, pp. 389–406, Mar. 1998.
[6] C. Jost, O. Arino, and R. Arditi, "About deterministic extinction in ratio-dependent predator–prey models," *Bull. Math. Biol.*, vol. 61, no. 1, pp. 19–32, Jan. 1999.
[7] S. Sarwardi, M. Haque, and P. K. Mandal, "Ratio-dependent predator–prey model of interacting population with delay effect," *Nonlinear Dyn.*, vol. 69, no. 3, pp. 817–836, Aug. 2012.
[8] Y. Song and X. Zou, "Bifurcation analysis of a diffusive ratio-dependent predator–prey model," *Nonlinear Dyn.*, vol. 78, no. 1, pp. 49–70, Oct. 2014.
[9] F. Berezovskaya, G. Karev, and R. Arditi, "Parametric analysis of the ratio-dependent predator-prey model," *J. Math. Biol.*, vol. 43, no. 3, pp. 221–246, Sep. 2001.
[10] K. Das, M. N. Srinivas, and N. Huda Gazi, "Diffusion dynamics and impact of noise on a discrete-time ratio-dependent model: An analytical and numerical approach," *Math. Comput. Appl.*, vol. 24, no. 4, p. 103, Dec. 2019.
[11] L. Cheng and H. Cao, "Bifurcation analysis of a discrete-time ratio-dependent predator–prey model with allee effect," *Commun. Nonlinear Sci. Numer. Simul.*, vol. 38, pp. 288–302, Sep. 2016.
[12] L. Zhang, J. Liu, and M. Banerjee, "Hopf and steady state bifurcation analysis in a ratio-dependent predator–prey model," *Commun. Nonlinear Sci. Numer. Simul.*, vol. 44, pp. 52–73, Mar. 2017.
[13] Z. Lajmiri, R. Khoshsiar Ghaziani, and I. Orak, "Bifurcation and stability analysis of a ratio-dependent predator-prey model with predator harvesting rate," *Chaos, Solitons Fractals*, vol. 106, pp. 193–200, Jan. 2018.
[14] Q. Din, "Qualitative analysis and chaos control in a density-dependent host–parasitoid system," *Int. J. Dyn. Control*, vol. 6, no. 2, pp. 778–798, Jun. 2018.
[15] M. S. Shabbir, Q. Din, R. Alabdan, A. Tassaddiq, and K. Ahmad, "Dynamical complexity in a class of novel discrete-time predator-prey interaction with cannibalism," *IEEE Access*, vol. 8, pp. 100226–100240, 2020.
[16] Z. He and X. Lai, "Bifurcation and chaotic behavior of a discrete-time predator-prey system," *Nonlinear Anal Real World Appl.*, vol. 12, no. 1, pp. 403–417, Feb. 2011.
[17] Z. Jing and J. Yang, "Bifurcation and chaos in discrete-time predator-prey system," *Chaos, Solitons Fractals*, vol. 27, no. 1, pp. 259–277, Jan. 2006.
[18] Q. Din, "Bifurcation analysis and chaos control in discrete-time glycolysis models," *J. Math. Chem.*, vol. 56, no. 3, pp. 904–931, Mar. 2018.
[19] J. Guckenheimer and P. Holmes, *Nonlinear Oscillations, Dynamical Systems, and Bifurcations of Vector Fields*. New York, NY, USA: Springer, 1983.
[20] C. Robinson, *Dynamical Systems: Stability, Symbolic Dynamics and Chaos*. New York, NY, USA: Boca Raton; 1999.
[21] S. Wiggins, *Introduction to Applied Nonlinear Dynamical Systems and Chaos*. New York, NY, USA: Springer, 2003.
[22] Y. H. Wan, "Computation of the stability condition for the hopf bifurcation of diffeomorphism on R^2," *SIAM J. Appl. Math.*, vol. 34, no. 1, pp. 167–175, Jan. 1978.
[23] Y. A. Kuznetsov, *Elements of Applied Bifurcation Theory*. New York, NY, USA: Springer, 1997.
[24] E. Ott, C. Grebogi, and J. A. Yorke, "Controlling chaos," *Phys. Rev. Lett.*, vol. 64, pp. 1196–1199, Mar. 1990.
[25] S. Lynch, *Dynamical Systems With Applications Using Mathematica*. Boston, MA, USA: Birkhäuser; 2007.
[26] X. S. Luo, G. Chen, B. H. Wang, and J. Q. Fang, "Hybrid control of period-doubling bifurcation and chaos in discrete nonlinear dynamical systems," *Chaos, Solitons Fractals*, vol. 18, no. 4, pp. 775–783, Nov. 2003.
[27] L.-G. Yuan and Q.-G. Yang, "Bifurcation, invariant curve and hybrid control in a discrete-time predator–prey system," *Appl. Math. Model.*, vol. 39, no. 8, pp. 2345–2362, Apr. 2015.
[28] M. S. Shabbir, Q. Din, M. Safeer, M. A. Khan, and K. Ahmad, "A dynamically consistent nonstandard finite difference scheme for a predator–prey model," *Adv. Difference Equ.*, vol. 2019, no. 1, pp. 1–17, Dec. 2019.
[29] Q. Din, M. S. Shabbir, M. A. Khan, and K. Ahmad, "Bifurcation analysis and chaos control for a plant–herbivore model with weak predator functional response," *J. Biol. Dyn.*, vol. 13, no. 1, pp. 481–501, Jan. 2019.
[30] X. Liu and D. Xiao, "Complex dynamic behaviors of a discrete-time predator–prey system," *Chaos, Solitons Fractals*, vol. 32, no. 1, pp. 80–94, Apr. 2007.
[31] R. E. Mickens, *Nonstandard Finite Difference Methods of Differential Equations*. Singapore: World Scientific, 1994.
[32] H. Al-Kahby, F. Dannan, and S. Elaydi, "Non-standard discretization methods for some biological models," in *Applications of Nonstandard Finite Difference Schemes*. Singapore: World Scientific, 2000, pp. 155–180.
[33] H. Baek, "Complex dynamics of a discrete-time predator-prey system with ivlev functional response," *Math. Problems Eng.*, vol. 2018, pp. 1–15, Jan. 2018.
[34] N. Bairagi and M. Biswas, "A predator-prey model with beddington-DeAngelis functional response: A non-standard finite-difference method," *J. Difference Equ. Appl.*, vol. 22, no. 4, pp. 581–593, Apr. 2016.
[35] Q. Chen, Z. Teng, and Z. Hu, "Bifurcation and control for a discrete-time prey–predator model with holling-IV functional response," *Int. J. Appl. Math. Comput. Sci.*, vol. 23, no. 2, pp. 247–261, Jun. 2013.
[36] Q. Cui, Q. Zhang, Z. Qiu, and Z. Hu, "Complex dynamics of a discrete-time predator-prey system with holling IV functional response," *Chaos, Solitons Fractals*, vol. 87, pp. 158–171, Jun. 2016.
[37] I. Darti and A. Suryanto, "Stability preserving non-standard finite difference scheme for a harvesting Leslie–Gower predator–prey model," *J. Difference Equ. Appl.*, vol. 21, no. 6, pp. 528–534, Jun. 2015.
[38] D. T. Dimitrov and H. V. Kojouharov, "Nonstandard finite-difference methods for predator–prey models with general functional response," *Math. Comput. Simul.*, vol. 78, no. 1, pp. 1–11, Jun. 2008.
[39] Q. Din, "Complexity and chaos control in a discrete-time prey-predator model," *Commun. Nonlinear Sci. Numer. Simul.*, vol. 49, pp. 113–134, Aug. 2017.
[40] Q. Din, "Controlling chaos in a discrete-time prey-predator model with allee effects," *Int. J. Dyn. Control*, vol. 6, no. 2, pp. 858–872, Jun. 2018.
[41] Q. Din, "Stability, bifurcation analysis and chaos control for a predator-prey system," *J. Vibrat. Control*, vol. 25, no. 3, pp. 612–626, Feb. 2019.
[42] H. Jiang and T. D. Rogers, "The discrete dynamics of symmetric competition in the plane," *J. Math. Biol.*, vol. 25, no. 6, pp. 573–596, Dec. 1987.
[43] Z. Jing and J. Yang, "Bifurcation and chaos in discrete-time predator–prey system," *Chaos, Solitons Fractals*, vol. 27, no. 1, pp. 259–277, Jan. 2006.
[44] W. Krawcewicz and T. D. Rogers, "Perfect harmony: The discrete dynamics of cooperation," *J. Math. Biol.*, vol. 28, no. 4, pp. 383–410, Jun. 1990.
[45] P. Liu and S. N. Elaydi, "Discrete competitive and cooperative models of Lotka-Volterra type," *J. Comput. Anal. Appl.*, vol. 3, no. 1, pp. 53–73, Jan. 2001.
[46] K. Rajagopal, A. Akgul, I. M. Moroz, Z. Wei, S. Jafari, and I. Hussain, "A simple chaotic system with topologically different attractors," *IEEE Access*, vol. 7, pp. 89936–89947, 2019.
[47] S. M. Moghadas, M. E. Alexander, and B. D. Corbett, "A non-standard numerical scheme for a generalized gause-type predator–prey model," *Phys. D, Nonlinear Phenomena*, vol. 188, nos. 1–2, pp. 134–151, Jan. 2004.
[48] M. Y. Ongun and N. Ozdogan, "A nonstandard numerical scheme for a predator-prey model with allee effect," *J. Nonlinear Sci. Appl.*, vol. 10, no. 02, pp. 713–723, Feb. 2017.
[49] L. I. Roeger and L. Allen, "Discrete May-Leonard competitive models I," *J. Differ. Equ. Appl.*, vol. 10, no. 2, pp. 77–98, Feb. 2004.
[50] L. I. Roeger, "Discrete May-Leonard competitive models II," *Discrete Cont. Dyn. B*, vol. 5, no. 3, pp. 841–860, Aug. 2005.
[51] L.-I.-W. Roeger, "Discrete May–Leonard competition models III," *J. Difference Equ. Appl.*, vol. 10, no. 8, pp. 773–790, Jul. 2004.
[52] S. Ushiki, "Central difference scheme and chaos," *Phys. D, Nonlinear Phenomena*, vol. 4, no. 3, pp. 407–424, Mar. 1982.
[53] M. S. Shabbir, Q. Din, K. Ahmad, A. Tassaddiq, A. H. Soori, and M. A. Khan, "Stability, bifurcation, and chaos control of a novel discrete-time model involving allee effect and cannibalism," *Adv. Difference Equ.*, vol. 2020, no. 1, pp. 1–28, Dec. 2020.
[54] Q. Din, "A novel chaos control strategy for discrete-time brusselator models," *J. Math. Chem.*, vol. 56, no. 10, pp. 3045–3075, Nov. 2018.
[55] H. Gritli and S. Belghith, "Walking dynamics of the passive compass-gait model under OGY-based state-feedback control: Rise of the Neimark–Sacker bifurcation," *Chaos, Solitons Fractals*, vol. 110, pp. 158–168, May 2018.

ASIFA TASSADDIQ (Member, IEEE) is currently an Associate Professor of mathematics with the College of Computer and Information Sciences, Majmaah University, Saudi Arabia. Her area of interest is mathematical analysis and applications. She has published several articles in reputed journals. She also has presented her research work in different conferences/workshops at national and international levels.

MUHAMMAD SAJJAD SHABBIR received the M.Phil. degree from the Mirpur University of Science and Technology MUST, Mirpur AJK, Pakistan, in 2015. He is currently pursuing the Ph.D. degree with Air University Islamabad, Pakistan. His current areas of research including stability analysis, bifurcation analysis, and chaos control in a discrete-time dynamical systems.

QAMAR DIN received the Ph.D. degree in discrete approximations and optimization of evolution inclusions and equations from the Abdus Salam School of Mathematical Science, GC University, Lahore, Pakistan, in 2012. He is currently a tenured Associate Professor with the Department of Mathematics, University of Poonch Rawalakot, Azad Jammu and Kashmir, Pakistan. His current research interests include stability analysis, bifurcation analysis, and chaos control in discrete-time systems. He has published more than 96 research articles in reputed international journals.

KHALIL AHMAD received the Ph.D. degree in geometric function theory of complex analysis from COMSATS University Islamabad, Pakistan, in 2014. He is currently an Assistant Professor with the Department of Mathematics, Air University Islamabad, Pakistan. His current research interests include stability analysis, bifurcation analysis and chaos control in discrete-time systems, approximation theory, and complex analysis.

SABEENA KAZI is currently an Assistant Professor of mathematics with the College of Computer and Information Sciences, Majmaah University, Saudi Arabia. Her area of interest is mathematical analysis and applications. She has published several articles in reputed journals and participated in national and international conferences.